Available online at www.sciencedirect.com

ScienceDirect

www.elsevier.com/locate/jes

JES JOURNAL OF ENVIRONMENTAL SCIENCES

www.jesc.ac.cn

Multiple transformation pathways of *p*-arsanilic acid to inorganic arsenic species in water during UV disinfection

Suqi Li[1], *Jing Xu*[1], *Wei Chen*[1], *Yingtan Yu*[1], *Zizheng Liu*[2,*], *Jinjun Li*[1,*], *Feng Wu*[1]

1. *Department of Environmental Science, School of Resources and Environmental Science, Wuhan University, Wuhan 430079, China. E-mail: 126120824@qq.com*

2. *School of Civil Engineering, Wuhan University, Wuhan 430072, China*

ARTICLE INFO

Article history:
Received 17 October 2015
Revised 20 January 2016
Accepted 22 January 2016
Available online 5 March 2016

Keywords:
p-Arsanilic acid
Phototransformation
Inorganic arsenic species
Kinetics
Mechanism

ABSTRACT

p-Arsanilic acid (*p*-ASA) is widely used in China as livestock and poultry feed additive for promoting animal growth. The use of organoarsenics poses a potential threat to the environment because it is mostly excreted by animals in its original form and can be transformed by UV–Vis light excitation. This work examined the initial rate and efficiency of *p*-ASA phototransformation under UV-C disinfection lamp. Several factors influencing *p*-ASA phototransformation, namely, pH, initial concentration, temperature, as well as the presence of NaCl, NH_4^+, and humic acid, were investigated. Quenching experiments and LC–MS were performed to investigate the mechanism of *p*-ASA phototransformation. Results show that *p*-ASA was decomposed to inorganic arsenic (including As(III) and As(V)) and aromatic products by UV-C light through direct photolysis and indirect oxidation. The oxidation efficency of *p*-ASA by direct photosis was about 32%, and those by HO. and $^1O_2$ were 19% and 49%, respectively. Cleavage of the arsenic–benzene bond through direct photolysis, HO. oxidation or $^1O_2$ oxidation results in simultaneous formation of inorganic As(III), As(IV), and As(V). Inorganic As(III) is oxidized to As(IV) and then to As(V) by $^1O_2$ or HO.. As(IV) can undergo dismutation or simply react with oxygen to produce As(V) as well. Reactions of the organic moieties of *p*-ASA produce aniline, aminophenol and azobenzene derivatives as main products. The photoconvertible property of *p*-ASA implies that UV disinfection of wastewaters from poultry and swine farms containing *p*-ASA poses a potential threat to the ecosystem, especially agricultural environments.

Introduction

The phenylarsonic (PA) compounds *p*-arsanilic acid (*p*-ASA) and roxarsone (ROX) have been used mainly as feed additives for promoting growth and as antibiotics for poultry and swine (Levander, 1977). Levels of *p*-ASA and ROX in antibiotics for pigs and chickens are about 45 and 30 mg/kg respectively (Straw et al., 2002). Yao et al. (2013) reported in a study of 146 animal feeds that 25.4% of them contained organoarsenics, with average arsenic levels of 21.2 and 7.0 mg/kg in the form of *p*-ASA and ROX, respectively. Most *p*-ASA or ROX that is ingested is excreted in its original chemical form (Morrison, 1969). Previous work about the potential risk of organic arsenic (Brown et al., 2005; Garbarino et al., 2003; Rutherford et al., 2003) was mainly focused on ROX due to several reports (Jackson and Bertsch, 2001; Jackson et al., 2003; Makris et al., 2008) that found that the concentration of *p*-ASA in some area in the United States is relatively low. However, *p*-ASA is

* *Corresponding authors*. E-mails: lzz@hust.edu.cn (Zizheng Liu), ljj0410@163.com (Jinjun Li).

http://dx.doi.org/10.1016/j.jes.2016.01.017
1001-0742/

widely used in swine farms in China, and its dosage in animal feeds is higher than that of ROX (Yao et al., 2013); *p*-ASA is known to remain as a residue in soil or in wastewater from swine farms. Recently, a study (Liu et al., 2014) has established *p*-ASA concentrations in environmental matrixes (surface soils, sediments, and surface waters) from dense swine farms in the Pearl River Delta (southern China). It is reported that *p*-ASA and inorganic As(V)/As(III) are the major arsenic species in these matrixes but ROX was not detectable. Interestingly, the environmental behavior and effect of *p*-ASA residues in swine farm wastes or agricultural soils amended with swine manure have drawn attention after a plague that killed pigs in Zhejiang Province in China in 2013 (Wang et al., 2014; Zhu et al., 2014). Great attention has been paid to the transformation of organic arsenic species into the more toxic inorganic forms, As(V) and As(III), because of seafood safety (Devesa et al., 2001). Such transformations are also the major fate of organoarsenic additives excreted into environments, resulting in increased concentrations of As(V) and As(III) in receiving waters or soils.

Solar photolysis has been thought to be the key process of abiotic degradation of organic arsenic species during waste storage or treatment (Jackson and Bertsch, 2001; Jackson et al., 2003; Makris et al., 2008). Bednar et al. (2003) proposed that As(III) can be photolytically cleaved from the ROX moiety at pH 4–8 by using radiation with 300 nm maximum emission line. They observed in this study the oxidation of As(III) to As(V). Arroyo-Abad et al. (2012) investigated the transformation of PA under irradiation with visible light by using a high-pressure mercury lamp with filter for wavelengths above 400 nm. They found that PA derivatives identified as various forms of hydroxyphenylarsonic acid appeared with increasing irradiation time. Zhu et al. (2014) investigated *p*-ASA photolysis under simulated sunlight by using a 500 W medium-pressure mercury lamp with wavelength above 290 nm. Citing the work of Bednar et al. (2003) they proposed that ionization of the phenolic groups of *p*-ASA intermediates produced by irradiation may result in the formation of electron-rich As–C bonds and may promote As(III) elimination from the aromatic ring. But the substrate in the study by Bednar et al. (2003) was ROX, which is different from *p*-ASA. Moreover, Bednar et al. (2003) only proposed a plausible mechanism of ROX photodegradation in the presence of nitrate through photolytic reductive cleavage of the As–C bond; they did not perform a detailed investigation on the exact mechanism of direct photolysis of *p*-ASA. *p*-ASA is very sensitive to ionizing radiation (*e.g.*, γ rays) and produces arsenate-centered radicals ([$(OH)_2As = O$].) (Karabulut and Tapramaz, 1999) as As(IV) intermediates. Xu et al. (2007) investigated the hydroxyl radical (HO.) oxidation of PA by γ radiolysis under conditions that generate HO.. They observed the initial formation of As(III) and As(V) at approximately 1:1 molar ratio, which was consistent with the disproportion of an As(IV) intermediate produced by homolytic cleavage of the As–C bond. Although the aforementioned works revealed the solar photochemical transformation of *p*-ASA to inorganic As(V) and As(III) in water, the mechanism of direct photolysis of *p*-ASA through As–C bond cleavage is still poorly understood.

A potentially important risk of *p*-ASA in swine farms has been ignored in previous studies. Ultraviolet (UV) disinfection has often been used in the wastewater treatment system (Lindenauer and Darby, 1994) and also for eliminating bacteria and viruses in poultry and swine farms (Turner and Burton, 1997). For this purpose, low-pressure mercury lamps with major emission at 254 nm wavelength are commonly used. When Czaplicka et al. (2014) did a short study on *p*-ASA photodegradation at low pH using a UV lamp with wavelength emission at 254 nm, they identified aniline as the main degradation product and proposed a possible mechanism based on the photolytic reductive cleavage of the As–C bond that generates aniline and inorganic arsenic compounds. However, they did not detect inorganic As(V) and As(III) species by any speciation methods and did not provide exact data on the distribution of inorganic As(V) and As(III).

Although the pathways for decomposition of *p*-ASA and production of inorganic arsenic are predictable, those of *p*-ASA photolysis during UV disinfection and their potential effects are still unknown. This study aims at helping in understanding the transformation behaviors during UV disinfection and the potential effect of the photolysis products of *p*-ASA on the receiving environments. All proposed reactions of the inorganic arsenic species involved and the scavenging reactions of reactive oxygen species (mainly HO. and $^1O_2$) are presented in Table 1.

1. Material and methods

1.1. Chemicals and reagents

p-ASA ($C_6H_8AsNO_3$, 98%) was purchased from Aladdin Industrial Corporation (Shanghai, China) and was used without any further purification. $Na_2HAsO_4{\cdot}7H_2O$ was purchased from Alfa Aesar (Ward Hill, MA, USA). Humic acid (HA, technical grade) was purchased from Sigma-Aldrich Co., Ltd. (St. Louis, MO, USA). Isopropyl alcohol (IPA, ≥99.9%) was purchased from Tianjin Kermel Chemical Reagent Co., Ltd., and furfuryl alcohol (FFA, 98%) was purchased from Shanghai Jinshan Tingxin Chemical Reagent Co., Ltd. All other reagents were analytically pure and were purchased from Sinopharm Chemical Reagent Co., Ltd. The real wastewater containing *p*-ASA was obtained from a swine farm at Jinmen City (Hubei Province, China) and was centrifuged at 12,000 r/min for 10 min before photolysis. Ultrapure water with 18 MΩ cm resistivity obtained through a water purification system (Liyuan Electric Instrument Co., Beijing, China) was used in all experiments. All prepared solutions were stored at 4°C and were protected from light.

1.2. Photochemical experiments

Fig. 1a depicts the structure of the photochemical reactor and the UV-C lamp used for disinfection. A cylinder hollow cooling equipment was used for the reaction and the parameters of reactor have been tagged in figure. The circulating cooling water was used to ensure the reaction conducted at desire temperature. An 8 W UV-C disinfection lamp (λ_{max} = 254 nm) was used as light source and was immersed in solution during the reaction. The parameters of UV-C lamp was shown in the right side, the light intensity was (4.5 ± 0.3) mW/cm^2 and the width of irradiation zone was 1.47 cm. Fig. 1b shows the light emission spectrum of UV-C lamp and the absorbance of *p*-ASA at various pH values. The lamp had several emission peaks and the strongest peak was

Table 1 – Summary of reactions between inorganic arsenic and oxidants that are possibly involved in UV disinfection, as well as reactions used for radical scavenging.

Reaction	k ((mol/L)$^{-1}$·sec^{-1})	References
$As(OH)_4 + As(OH)_4 \rightarrow As(V)(OH)_5 + As(III)(OH)_3$	8.4×10^8	Klaening et al. (1989)
$As(III)(OH)_3 + HO. \rightarrow As(IV)(OH)_4$	8.5×10^9	Dutta et al. (2005)
$As(IV)(OH)_4 + HO. \rightarrow H_2As(V)O_4^- + H_3O^+$	very fast	Lee and Choi (2002)
$As(IV)(OH)_4 + O_2 \rightarrow As(V) + O_2^-.$	1.4×10^9	Klaening et al. (1989)
$As(OH)_3O^- + O_2 \rightarrow As(V) + O_2^-.$	1.1×10^9	Klaening et al. (1989)
HO. + isopropanol → product	1.9×10^9	Buxton et al. (1988)
$^1O_2$ + FFA → products	1.4×10^8	Gottfried and Kimel (1991)
Furfuryl alcohol + HO. → addition	1.5×10^{10}	Savel'eva et al. (1972)

at 254 nm. The lamp also had several emission peaks in the range of 290–400 nm, while the absorbance of *p*-ASA was very weak over this range of wavelengths.

The concentration of *p*-ASA stock solution was 289.41 mg/L. 2.5 mL of *p*-ASA stock solution was added to a 500 mL-flask and then diluted with ultrapure water. The resulting solution was placed in the cooling equipment after it was blended well. Dilute H_2SO_4 and NaOH solutions were used to adjust the solution to the desired pH value, and then the lamp was switched on. The solutions were stirred continuously by using a magnetic stirrer. At specified intervals, a sample of the solution was collected for analysis. The content of dissolved oxygen in the solution was 6 mg/L. In the N_2 purging experiment, the top of the cylinder reactor was sealed with a rubber stopper. The solution was purged with high-purity N_2 (99.99%) for 30 min before photolysis and was retained during photolysis. Experiments involving addition of isopropyl alcohol (IPA) and furfuryl alcohol (FFA) were conducted to investigate the contribution of HO. and $^1O_2$, respectively, with the IPA or FFA dosages being 2000 times that of the initial *p*-ASA mole concentration.

In real wastewater phototransformation experiments, 500 mL of real wastewater from swine farm was used instead of simulated *p*-ASA containing wastewater for reaction, other procedures was the same as mentioned above.

1.3. Analytical methods

Analysis of inorganic arsenic was conducted by using hydride generation atomic fluorescence spectrometry (HG-AFS, Jitian Instrument Co. Ltd., Beijing, China). The analytical method for determination of total concentration of inorganic arsenic was based on our previous work (Xu et al., 2013; Wang et al., 2013). Experiments were conducted at least twice and results are shown as mean values with error bars. The limit detection and precision of HG-AFS was discussed in detail in the reports of Ren et al. (2011) and Liao and Deng (2006), the influence of As(V) during As(III) determination was subtracted by making standard curve at different ratios of As(III) and As(V).

The *p*-ASA concentration was determined by high-performance liquid chromatography (HPLC, Shimadzu Instrument Co. Ltd., Japan) at 25°C using a 10ADVP pump, an SPD-10AVP detector, and a C18 column (Supelco Discovery, 4.6 mm × 250 mm, 5 um). The detector wavelength was 254 nm, and the retention time was 4.2 min. The mobile phase was a 2.5% formic acid/methanol solution (95:5, V/V), and the flow rate was 1.0 mL/min. The detection limit (DL) of analytical method for *p*-ASA and precision of the used analytical methods was 6.29 μg/L and 0.48% respectively.

Products were identified by liquid chromatography–mass spectrometry (LC–MS, Agilent Technologies Co. Ltd., China) using an electrospray ionization ion source under positive mode. The ionization dry temperature was 350°C. The nebulizer pressure, dry gas flow rate, and HV capillary voltage were set at 40.00 psi, 10.00 L/min, and 4000 V, respectively. The column and mobile phase used for LC–MS were the same as those for HPLC. The sample was concentrated by vacuum freeze-drying and then redissolved in several milliliters of deionized water.

In UV–Vis absorption spectroscopic experiments, the reaction was conducted in a 10 cm quartz cuvette at room temperature. A glass rod was used to stir the solution during

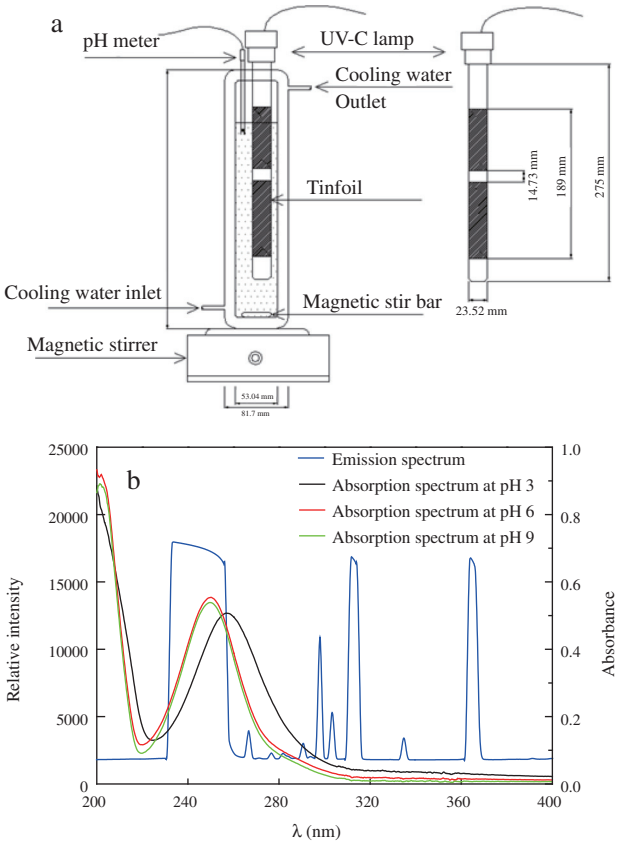

Fig. 1 – Photochemical reactor (a) and (b) light emission spectrum of UV-C lamp used for disinfection and absorbance of 1.45 mg/L *p*-Arsanilic acid (*p*-ASA) at various pH values.

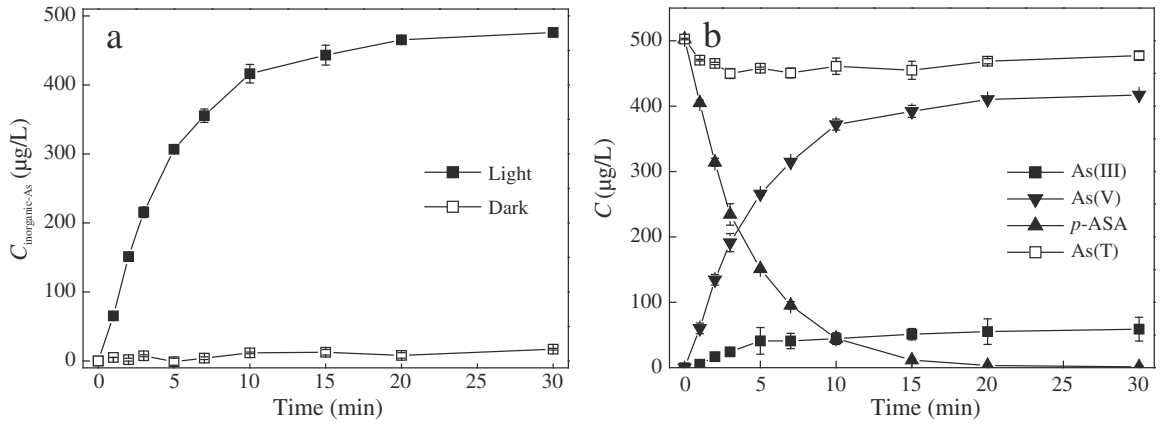

Fig. 2 – Changes in inorganic arsenic concentration with reaction time at dark and light conditions (a). Initial *p*-ASA concentration = 1.45 mg/L, initial pH = 6, temperature = 20°C. Mass balance and concentration changes of simulated wastewater in each arsenic species with reaction time (b). The concentration in figure is expressed in terms of atoms of inorganic arsenic. Initial *p*-ASA concentration = 1.45 mg/L, initial pH = 6, temperature = 20°C.

the reaction. Each sample was analyzed in a spectrophotometer (UV-1601, Shimadzu, Japan) over a wavelength range of 200–800 nm. Total organic carbon (TOC) was determined by using a multi N/C 2100 TOC analyzer (Jena, Germany).

2. Results and discussion

2.1. Mass balance of arsenic species during aerobic phototransformation of *p*-ASA

Experiments were conducted at pH 6 to investigate the transformation of *p*-ASA under both light and dark conditions (results are shown in Fig. 2a). In the dark condition, no transformation of *p*-ASA was observed within 30 min. In contrast, the increase in inorganic arsenic content under UV-C irradiation within the same period was significant; 90% of *p*-ASA was converted into the inorganic form in 15 min. Meanwhile, the amounts of *p*-ASA and inorganic As(III), As(V) were also determined to investigate the mass balance of the phototransformation reaction. As shown in Fig. 2b, under the irradiation of UV-C light at pH 6, the concentration of *p*-ASA decreased, and that of inorganic arsenic increased simultaneously. Among the inorganic arsenic species, the amount of As(V) was much higher than that of As(III). However, the total amount of arsenic (calculated from the sum of As(III), As(V), and *p*-ASA concentrations) decreased slightly during the first 5 min and remained stable afterward. This behavior indicates that unknown organic arsenic species (<10%) formed during photolysis.

Phototransformation experiments for the real swine wastewater were also conducted (Fig. 3). The initial concentration of *p*-ASA in the real swine wastewater was 0.1 mg/L that is lower than those in the simulated wastewater used in this work. After 30 min irradiation, 35% of *p*-ASA was phototransformed and the concentration of inorganic arsenic in solution was 5.29 μg/L and 5.70 μg/L for As(III) and As(V) respectively. The phototransformation efficiency of the real wastewater is much lower than that in the simulated wastewater, which might be due to the complicated components in the real wastewater that contained multiple organic substances. This result verified the occurrence of *p*-ASA in swine farm wastewater and the existence of its transformation during UV disinfection.

2.2. Reaction kinetics and effect of temperature

The effect of initial *p*-ASA concentration C_0 (289.41, 578.83, 1447.07, 2315.31 and 2894.13 μg/L) on the initial phototransformation rate r_0 was investigated at pH 6 and 20°C. The initial rate r_0 was calculated in terms of the generation rate of total inorganic arsenic from the first four points during the time of photolysis (0, 1, 2, and 3 min; results are shown in Fig. 4). The first-order kinetic model was used to fit the results. The kinetic equation that we obtained is $r_0 = (0.046 \pm 0.002)\ C_0$ ($R^2 = 0.9938$). The observed reaction rate constant (k) was 0.046 min^{-1}, and the half-life of *p*-ASA found under this condition was 3.77 min.

The effect of temperature on the initial rate of *p*-ASA phototransformation is shown in Fig. 5. The experiments

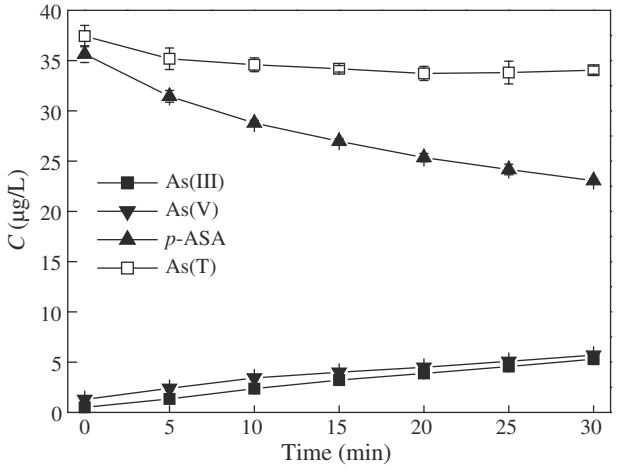

Fig. 3 – Mass balance and concentration changes of real swine wastewater in each arsenic species with reaction time. The concentration in figure is expressed in terms of atoms of inorganic arsenic. Initial *p*-ASA concentration = 0.1 mg/L, initial pH = 6, temperature = 20°C.

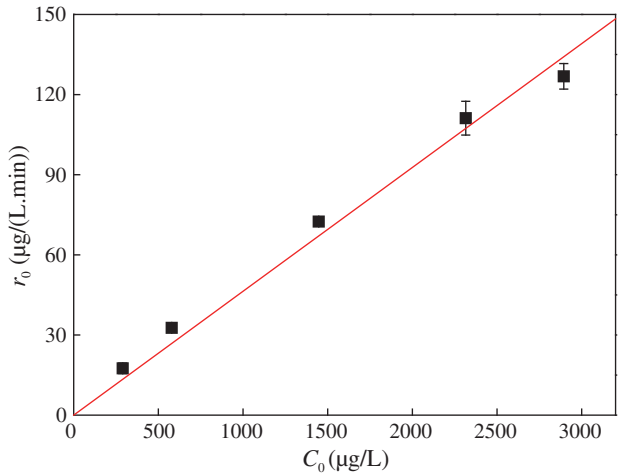

Fig. 4 – Kinetics of *p*-ASA phototransformation under 254 nm light. Initial pH = 6, temperature = 20°C.

demonstrated that the initial phototransformation rate was highly related to the temperature over the range of 10–30°C. Since direct photolysis is usually independent of the reaction temperature, results for temperature effects imply that aerobic *p*-ASA phototransformation was not a simple direct photolytic process, as confirmed later by radical-scavenging experiments.

2.3. *Effect of initial pH value, halide ion, ammonia, and humic acid*

Fig. 6a shows the changes in inorganic arsenic concentration at various initial pH values under of UV-C irradiation, indicating that pH value had a significant effect on the initial rate of *p*-ASA phototransformation. The initial phototransformation rate was 67.8 μg/(L·min) at pH 7 and increased to 100.6 μg/(L·min) at pH 9. At high pH, *p*-ASA mainly exists as a negatively charged ion (pK_{a1} 2.00, pK_{a2} = 4.02, pK_{a3} = 8.92 (Pergantis, 1997)) and can therefore easily ionize during phototransformation. The final

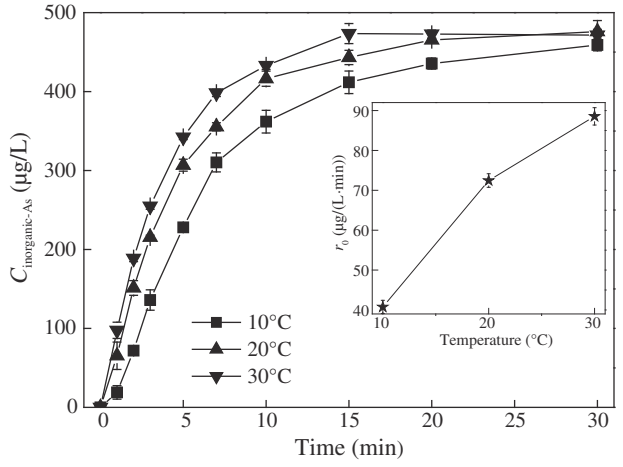

Fig. 5 – Initial rate and efficiency of *p*-ASA transformation under 254 nm light at various working temperatures. Initial *p*-ASA concentration = 1.45 mg/L, initial pH = 6°C.

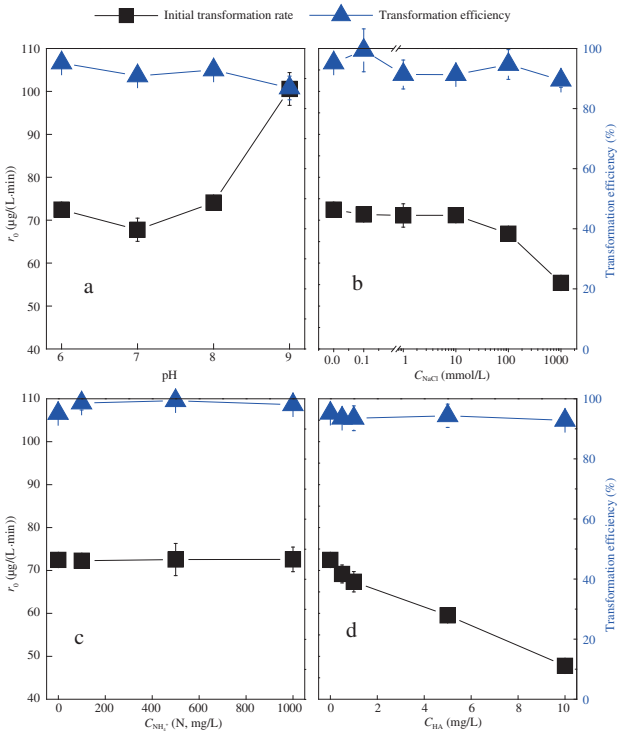

Fig. 6 – Initial rate and efficiency of *p*-ASA transformation under 254 nm light at various initial concentrations of H^+ (a), halide ion (b), ammonia nitrogen (c), and HA (d). Initial *p*-ASA concentration = 1.45 mg/L, initial pH = 6 (except in Fig. 6a), temperature = 20°C.

efficiencies of *p*-ASA transformation at 30 min at each pH value were similar, each approaching 100%. This result suggests that the pH value of the solution did not affect the final transformation efficiency and that organic arsenic could convert totally into the inorganic form.

Halide ion, ammonia nitrogen, and HA are widespread in livestock and poultry farms or in environments that are close to them; therefore, the effects of these substances on the phototransformation rate were investigated. NaCl, a typical halide salt, was used to investigate the effect of halide ion (results are shown in Fig. 6b). In the concentration range of 0.1 to 10 mmol/L, Cl^- did not show any obvious effect on the initial rate of *p*-ASA transformation; but when the concentration of Cl^- reached 1000 mmol/L, the initial transformation rate decreased from 72.5 to 55.4 μg/(L·min). The occurrence of Cl^- could react with free radicals (eg. $Cl^- + HO\cdot \rightarrow ClOH^-$, $k = 4.3 \pm 0.4 \times 10^9$ L/(mol·sec) (Jayson et al., 1973)) and thus decrease the transformation rate by competing with *p*-ASA. Moreover, halide ion and its derivate might affect the formation and stability of aromatic intermediates and thus reduce the mineral efficiency of arsenic by halogenating benzene ring (Price, 1941). The presence of Cl^- at 0.1 to 1000 mmol/L did not affect the final efficiency of *p*-ASA transformation (100%). This result implies that though excess Cl^- ions might inhibit indirect photolysis by scavenging HO. radicals or other pathways. The effect of ammonia (NH_4^+) at concentrations of 0–1000 mg/L (the concentration is expressed in terms of atoms of nitrogen) on *p*-ASA phototransformation at pH 6 was determined. Results in Fig. 6c

show that the presence of NH_4^+ did not affect the initial rate of *p*-ASA phototransformation and the final transformation efficiency. Results for the effect HA effect in Fig. 6d indicate that HA also reduced the rate of *p*-ASA phototransformation. In the range of 0–10 mmol/L, the inhibition effect shows a linear relationship with the HA concentration. The presence of HA did not affect the final efficiency of *p*-ASA transformation as well. Therefore, the decrease in the initial rate might be mainly due to absorption of UV-C light by HA, and the sufficiently long irradiation time (30 min) could compensate for the reduction of light absorption of *p*-ASA in the presence of HA.

2.4. Variations of UV–Vis spectra and TOC

UV–Vis spectra were obtained to investigate the change in absorbance of the solution during the reaction. Absorption spectra obtained by scanning from 200 to 800 nm during the 30 min reaction are shown in Fig. 7. At the start of the reaction, *p*-ASA showed characteristic peaks only at 220 and 252 nm. Along with the phototransformation of *p*-ASA, a characteristic peak emerged at 521 nm. The inset of the two figures depicts the transition of the absorbance at 521 and 252 nm. The absorbance at 521 nm increased within the first 10 min and decreased afterward. This behavior indicates that azo products formed in this system and underwent transformation afterward upon UV-C irradiation. The generation of azo products was also confirmed in LC–MS results which will be discussed later. The characteristic absorption peak at 252 nm, which represents the benzene ring (Han et al., 2004), its intensity decreased initially and then reached a plateau, indicating that the benzene ring was intact during the reaction and that initial changes were due to transformation of the bond between arsenic and the benzene ring (i.e., As–C bond).

To determine the variation of organic constituents of the sample, TOC experiments were conducted. As shown in Fig. 8, 96.3% of *p*-ASA was degraded, while the TOC did not change obviously. The results also prove that the organic moiety of *p*-ASA was intact during UV-C irradiation.

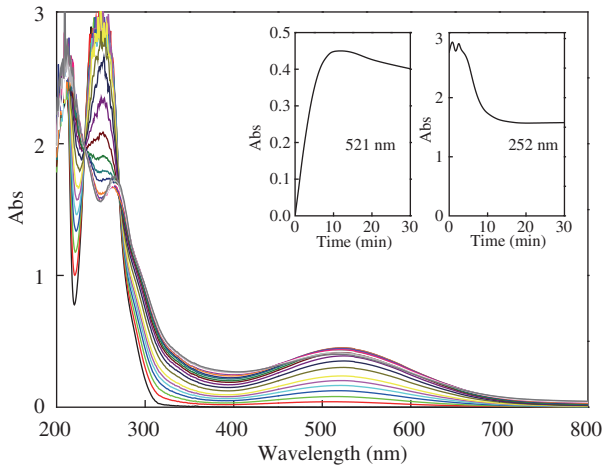

Fig. 7 – Change in *p*-ASA absorbance at characteristic wavelengths during 30 min photoreaction. Initial *p*-ASA concentration = 7.24 mg/L, initial pH = 6.

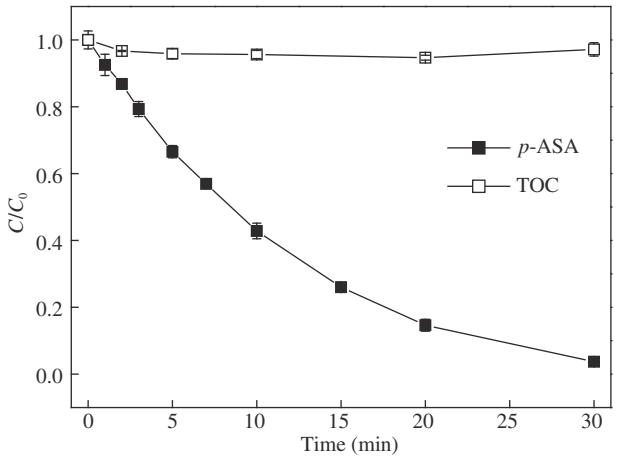

Fig. 8 – Changes in *p*-ASA concentration and total organic carbon (TOC) under 254 nm light. Initial *p*-ASA concentration = 1.45 mg/L, initial pH = 6, temperature = 20°C.

2.5. Mechanism of *p*-ASA transformation under UV-C irradiation

To investigate the mechanism of *p*-ASA phototransformation in this system, we conducted experiments involving addition of various inhibitors. N_2 purging was done before and during the reaction that was used for investigation of direct photolysis. IPA and FFA were used to quench HO. and $^1O_2$. Both the decrease in the *p*-ASA content and the increase in levels of inorganic arsenic (As(III) and As(V)) were determined. As shown in Fig. 9, the degradation rate under the N_2 atmosphere was much higher than that under air condition. This demonstrates that under UV-C irradiation, *p*-ASA could undergo excitation to the *p*-ASA* state under a N_2 atmosphere and that *p*-ASA* undergoes direct photolysis to aniline and inorganic arsenic. In the presence of O_2, *p*-ASA* could excite O_2, generating $^1O_2$, which would revert to the ground state and thereby lower the phototransformation rate. Observed rate constants of *p*-ASA under different conditions are shown in

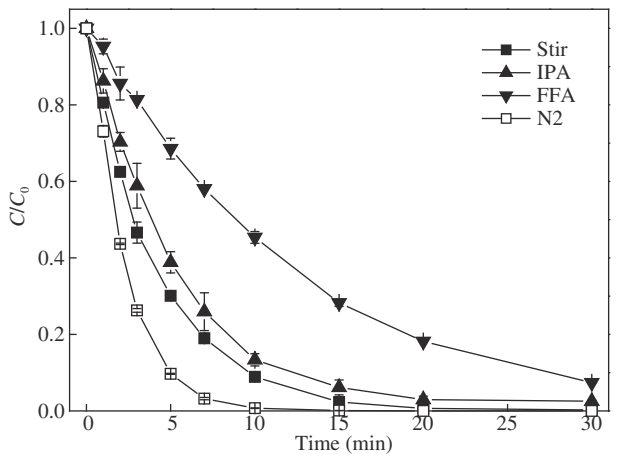

Fig. 9 – Changes in *p*-ASA concentration under 254 nm light with different quenchers. Initial *p*-ASA concentration = 1.45 mg/L, initial pH = 6, temperature = 20°C.

Table 2 – Observed rate constants of *p*-ASA and r_0 of inorganic arsenic under different conditions.

	k_{obs} of *p*-ASA (initial 10 min)	$k_{obs}/k_{obs,Air}$	$r_{0As(III)}$ (μg/(L·min))	$r_{0As(V)}$ (μg/(L·min))	$r_{0As(V)}/r_{0As(III)}$
Air	0.241 ± 0.009	100%	8.0 ± 0.5	64.5 ± 1.0	8.1
IPA	0.196 ± 0.018	81.3%	7.7 ± 0.7	60.0 ± 1.0	7.9
FFA	0.078 ± 0.000	32.3%	4.1 ± 0.5	26.4 ± 0.2	6.4
N_2	0.484 ± 0.010	/	35.6 ± 1.8	89.0 ± 1.3	2.5

Table 2, and the calculated relative contributions of direct or indirect (HO. or $^1O_2$) photolysis are shown in Table 3. Results show that in the quencher experiment, the degradation rate decreased by 18.7% and 67.7% in the presence of IPA or FFA, respectively, indicating that only 32.3% of *p*-ASA transformation under air was due to direct photolysis, while 18.7% was due to generated HO., and the remaining 49.0% was due to generated $^1O_2$.

The initial rates of As(III) and As(V) generation were also investigated (Table 2). Results show that As(III) comprised 28.6% of the inorganic arsenic that initially formed in the absence of oxygen. Upon irradiation, *p*-ASA generated As(III), As(V), and As(IV) simultaneously, and the generated intermediate As(IV) underwent disproportionation reaction to As(III) and As(V) (Klaening et al., 1989). Therefore, both As(III) and As(V) were detectable. In the presence of oxygen, more As(V) than As(III) was generated during *p*-ASA phototransformation; only 11.3%–13.4% of generated inorganic arsenic was As(III), and the rest was As(V). Indeed, in the presence of oxygen, a condition in which HO. and $^1O_2$ exist, As(III) and As(IV) can be oxidized quickly to As(V) (Klaening et al., 1989; Dutta et al., 2005; Lee and Choi, 2002), therefore decreased the observed generation rate of As(III). As mentioned above, the effect of HO. in this system was minimal; thus, the As(V)/As(III) ratio changed slightly during addition of IPA and changed more during FFA addition than it did during IPA addition because the contribution of $^1O_2$ was greater than that of HO.. Although the generated HO. and $^1O_2$ could be quenched by FFA, oxygen could still affect the pathway for inorganic arsenic and lead to the oxidation of As(III) and As(IV) (Klaening et al., 1989). Therefore, the As(V)/As(III) ratios in these systems were much higher than those in systems purged with N_2.

Table 3 – The relative contribution of direct or indirect photolysis.

Pathways		Relative contribution	Calculation equations
p_{direct}(%)		32.3%	$p_{direct} = \frac{k_{obs,FFA}}{k_{obs,Air}}$
$p_{indirect}$(%)	$p_{1_{O2}}$ (%)	49.0%	$p_{1_{O2}} = \frac{k_{obs,IPA}}{k_{obs,Air}} - p_{direct}$
	p_{HO} (%)	18.7%	$p_{HO} = 1 - p_{direct} - p_{1_{O2}}$

p denotes the contribution of specific pathway to the total photolysis rate of p-ASA. $k_{obs,FFA}$, $k_{obs,\ Air}$, $k_{obs,IPA}$ denote the observed rate of *p*-ASA in the presence of FFA, air (stirring), or IPA respectively.

2.6. Product identification and proposed pathways of *p*-ASA phototransformation

The total ion chromatography (TIC) of LC–MS results are shown in Fig. 10 and identified products are shown in Table 4. At 3.0 min, aminophenol, the tentative derivative of aniline oxidized by $^1O_2$ (Briviba et al., 1993) and HO. (Canel et al., 2005), was detected. Substances detected at 6.2 and 13.9 min, tentatively designated as 4-(2-phenyldiazenyl)phenylarsonic and hydroxyazobenzene, respectively, are derivatives of aminophenol (Farhadi et al., 2007; Laha and Luthy, 1990). The presence of an azo compound explains the characteristic peak at 521 nm. Notably, in experiments using stirring and involving IPA addition, the solution showed absorbance at 521 nm. In contrast, experiments involving N_2 purging and addition of FFA solution did not show obvious absorbance at the same wavelength. This difference indicates that azo compounds could emerge only with the generation of aminophenol. *p*-ASA was detected at 4.2 min, while a substance with an identical *m/z* ratio was detected at 11.5 min, suggesting an isomer of *p*-ASA. The generation of the isomer and the substances at 3.9 min (4-aminohydroxyphenylarsonic acid) and 6.2 min (4-(2-phenyldiazenyl)phenylarsonic acid), which contain the arsenic acid group, could explain the variability of the total amount of arsenic in Fig. 1.

The proposed pathways of *p*-ASA transformation are shown in Scheme 1. Upon UV-C irradiation, *p*-ASA undergoes three different pathways of decomposition. $^1O_2$ transforms 49.0% of *p*-ASA, and HO. transforms 18.7%. The remaining 32.3% of *p*-ASA undergoes direct photolysis mainly via excitation to *p*-ASA* followed by cleavage of the As–C bond. *p*-ASA* could also react with oxygen, thereby generating $^1O_2$, and subsequently deactivating. Cleavage of the arsenic–benzene bond results in simultaneous formation of inorganic As(III), As(IV), and As(V). $^1O_2$ or HO. oxidizes As(III) to As(IV), and As(IV) oxidizes to As(V) subsequently. As(IV) can undergo dismutation, generating As(V)

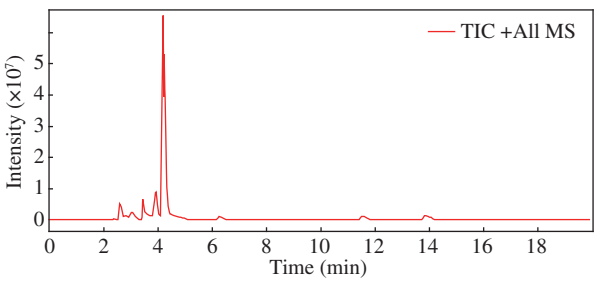

Fig. 10 – The total ion chromatography (TIC) of LC–MS.

Table 4 – Photolysis products in the presence of air during UV disinfection identified by LC–MS.

Retention time (min)	*m*/z	Chemicals	
		Appellation	Structure
3.0–3.1	109.7	Aminophenol	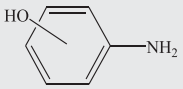
3.0–3.5	142.5–142.7	H_3AsO_4	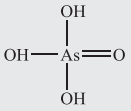
3.9	233.6	4-Amino-hydroxyphenylarsonic acid (HO-PAA)	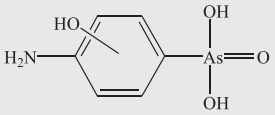
4.2	217.5	*p*-ASA	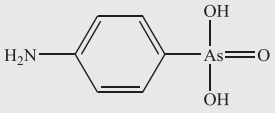
6.2	308.7	4-(2-Phenyldiazenyl)phenylarsonic acid	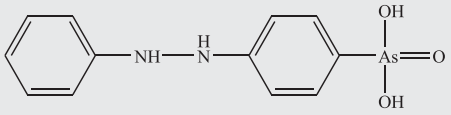
11.5	217.7	*o*-ASA	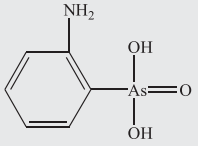
13.9	199.8	Hydroxy-azo-benzene	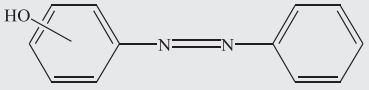

and As(III) or can simply react with oxygen, producing As(V) as well. Reactions of the organic moieties of *p*-ASA during UV photolysis are more complex. Upon cleavage of the As–C bond, aniline is obtained as the initial product. Part of the aniline is then oxidized by $^1O_2$ and/or HO. to aminophenol. Aniline and aminophenol undergo different pathways, forming other organic substances like azobenzene derivatives.

3. Conclusions

The phototransformation rate of *p*-ASA is affected by its initial concentration, solution pH, ionic strength, temperature and HA concentration, while the occurrence of ammonia does not pose influence on the transformation rate. Moreover, *p*-ASA

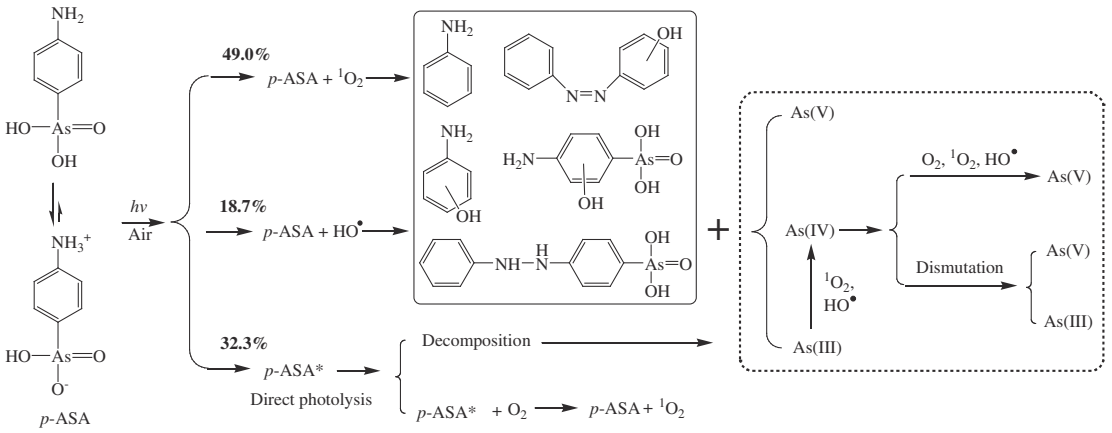

Scheme 1 – Proposed pathways of *p*-ASA transformation in solution at pH 6 during UV disinfection.

can be eventually transformed to inorganic form at those various conditions.

With the irradiation of UV-C light, 32.3% of *p*-ASA was decomposed by direct photolysis, and 18.7% and 49.0% was decomposed via oxidation by HO. and $^1O_2$, respectively. Cleavage of the arsenic–benzene bond results in the simultaneous formation of inorganic As(III), As(IV), and As(V), and then As(III) and As(IV) can be oxidized to As(V) in the presence of oxygen. Organic moieties such as aniline, aminophenol and azobenzene derivatives were also generated during phototransformation reaction.

p-ASA can pose a significant threat by transforming to higher toxic form (inorganic As(III) and As(V)) under the irradiation of UV-C light in farmland environment or during wastewater treatment, and eventually introduce arsenic into agricultural environment and can lead to arsenic accumulation. Therefore gradual decrease and eventual cessation of the use of PA compounds is imperative. Technologies for the removal of inorganic arsenic after UV-C disinfection and for end-of-the-pipe control of *p*-ASA-related contamination, such as adsorption and precipitation, should be considered.

Acknowledgment

This work was supported by the National Natural Science Foundation of China (Nos 51508423 and 21477090).

REFERENCES

Arroyo-Abad, U., Mattusch, J., Möder, M., Elizalde-Gomzalez, M.P., Matysik, F., 2012. Identification of degradation products of phenylarsonic acid and *o*-arsanilic acid in contact with suspensions of soils of volcanic origin. Talanta 99, 310–315.

Bednar, A.J., Garbarino, J.R., Ferrer, I., Rutherford, D.W., Wershaw, R.L., Ranville, J.F., et al., 2003. Photodegradation of roxarsone in poultry litter leachates. Sci. Total Environ. 302 (1), 237–245.

Briviba, K., Devasagayam, T.P., Sies, H., Steenken, S., 1993. Selective para-hydroxylation of phenol and aniline by singlet molecular oxygen. Chem. Res. Toxicol. 6 (4), 548–553.

Brown, B.L., Slaughter, A.D., Schreiber, M.E., 2005. Controls on roxarsone transport in agricultural watersheds. Appl. Geochem. 20 (1), 123–133.

Buxton, G.V., Greenstock, C.L., Helman, W.P., Ross, A.B., 1988. Critical review of rate constants for reactions of hydrated electrons, hydrogen atoms and hydroxyl radicals (.OH/.O– in aqueous solution. J. Phys. Chem. Ref. Data 17 (2), 513–886.

Canel, L.M., Santaballa, J.A., Vulliet, E., 2005. On the mechanism of TiO 2-photocatalyzed degradation of aniline derivatives. J. Photochem. Photobiol. A Chem. 175 (2), 192–200.

Czaplicka, M., Bratek, Ł., Jaworek, K., Bonarski, J., Pawlak, S., 2014. Photo-oxidation of *p*-arsanilic acid in acidic solutions: Kinetics and the identification of by-products and reaction pathways. Chem. Eng. J. 243, 364–371.

Devesa, V., Martinez, A., Suner, M.A., Benito, V., Vélez, D., Montoro, R., 2001. Kinetic study of transformations of arsenic species during heat treatment. J. Agric. Food Chem. 49 (5), 2267–2271.

Dutta, P.K., Pehkonen, S.O., Sharma, V.K., Ray, A.K., 2005. Photocatalytic oxidation of arsenic(III): evidence of hydroxyl radicals. Environ. Sci. Technol. 39 (6), 1827–1834.

Farhadi, S., Zaringhadam, P., Sahamieh, R.Z., 2007. Photo-assisted oxidation of anilines and other primary aromatic amines to azo compounds using mercury (II) oxide as a photo-oxidant. Acta Chim. Slov. 54 (3), 647.

Garbarino, J.R., Bednar, A.J., Rutherford, D.W., Beyer, R.S., Wershaw, R.L., 2003. Environmental fate of roxarsone in poultry litter. I. Degradation of roxarsone during composting. Environ. Sci. Technol. 37 (8), 1509–1514.

Gottfried, V., Kimel, S., 1991. Temperature effects on photosensitized processes. J. Photochem. Photobiol. B Biol. 8 (4), 419–430.

Han, W., Zhu, W., Zhang, P., Ying, Z., Li, L., 2004. Photocatalytic degradation of phenols in aqueous solution under irradiation of 254 and 185 nm UV light. Catal. Today 90 (3), 319–324.

Jackson, B.P., Bertsch, P.M., 2001. Determination of arsenic speciation in poultry wastes by IC-ICP-MS. Environ. Sci. Technol. 35 (24), 4868–4873.

Jackson, B.P., Bertsch, P.M., Cabrera, M.L., Camberato, J.J., Seaman, J.C., Wood, C.W., 2003. Trace element speciation in poultry litter. J. Environ. Qual. 32 (2), 535–540.

Jayson, G.G., Parsons, B.J., Swallow, A.J., 1973. Some simple, highly reactive, inorganic chlorine derivatives in aqueous solution. Their formation using pulses of radiation and their role in the mechanism of the Fricke dosimeter. J. Chem. Soc. Faraday Trans. 1 (69), 1597–1607.

Karabulut, B., Tapramaz, R., 1999. EPR study of gamma irradiated arsanilic acid single crystal. Radiat. Phys. Chem. 55 (3), 331–335.

Klaening, U.K., Bielski, B.H., Sehested, K., 1989. Arsenic (IV). A pulse-radiolysis study. Inorg. Chem. 28 (14), 2717–2724.

Laha, S., Luthy, R.G., 1990. Oxidation of aniline and other primary aromatic amines by manganese dioxide. Environ. Sci. Technol. 24 (3), 363–373.

Lee, H., Choi, W., 2002. Photocatalytic oxidation of arsenite in TiO_2 suspension: kinetics and mechanisms. Environ. Sci. Technol. 36 (17), 3872–3878.

Levander, O.A., 1977. Biological effects of arsenic on plants and animals: Domestic animals: Phenylarsonic feed additives. Arsenic: Medical and biological effects of environmental pollutants. National Academies Press, Washington DC, pp. 149–151.

Liao, M., Deng, T., 2006. Arsenic species analysis in porewaters and sediments using hydride generation atomic fluorescence spectrometry. J. Environ. Sci. 18 (5), 995–999.

Lindenauer, K.G., Darby, J.L., 1994. Ultraviolet disinfection of wastewater: Effect of dose on subsequent photoreactivation. Water Res. 28 (4), 805–817.

Liu, X., Zhang, W., Hu, Y., Hu, E., Xie, X., Wang, L., et al., 2014. Arsenic pollution of agricultural soils by concentrated animal feeding operations (CAFOs). Chemosphere 119, 273–281.

Makris, K.C., Quazi, S., Punamiya, P., Sarkar, D., Datta, R., 2008. Fate of arsenic in swine waste from concentrated animal feeding operations. J. Environ. Qual. 37 (4), 1626–1633.

Morrison, J.L., 1969. Distribution of arsenic from poultry litter in broiler chickens, soil, and crops. J. Agric. Food Chem. 17 (6), 1288–1290.

Pergantis, S.A., 1997. Speciation of arsenic animal feed additives by microbore high-performance liquid chromatography with inductively coupled plasma mass spectrometry. Analyst 122 (10), 1063–1068.

Price, C.C., 1941. Substitution and orientation in the benzene ring. Chem. Rev. 29 (1), 37–67.

Ren, C., Peng, H., Huang, W., Wang, Y., Wu, F., 2011. Speciation of inorganic As(V)/As(III) in water and soil by hydride generation atomic fluorescence spectrometry. Fresenius Environ. Bull. 20 (4), 1069–1074.

Rutherford, D.W., Bednar, A.J., Garbarino, J.R., Needham, R., Staver, K.W., Wershaw, R.L., 2003. Environmental fate of roxarsone in poultry litter. Part II. Mobility of arsenic in soils amended with poultry litter. Environ. Sci. Technol. 37 (8), 1515–1520.

Savel'eva, O.S., Shevchuk, L.G., Vysotskaya, N.A., 1972. Reactivity of substituted benzenes, furans, and pyridines to hydroxyl radicals. J. Org. Chem. USSR 8, 283–286.

Straw, B., Dewey, C., Kober, J., Henry, S.C., 2002. Factors associated with death due to hemorrhagic bowel syndrome in two large commercial swine farms. J. Swine Health Prod. 10 (2), 75–80.
Turner, C., Burton, C.H., 1997. The inactivation of viruses in pig slurries: A review. Bioresour. Technol. 61 (1), 9–20.
Wang, Y., Xu, J., Li, J., Wu, F., 2013. Natural montmorillonite induced photooxidation of As (III) in aqueous suspensions: Roles and sources of hydroxyl and hydroperoxyl/superoxide radicals. J. Hazard. Mater. 260, 255–262.
Wang, H.L., Hu, Z.H., Tong, Z.L., Xu, Q., Wang, W., Yuan, S., 2014. Effect of arsanilic acid on anaerobic methanogenic process: Kinetics, inhibition and biotransformation analysis. Biochem. Eng. J. 91, 179–185.
Xu, T., Kamat, P.V., Joshi, S., Mebel, A.M., Yong, C., O'Shea, K.E., 2007. Hydroxyl radical mediated degradation of phenylarsonic acid. J. Phys. Chem. A 111 (32), 7819–7824.
Xu, J., Li, J., Wu, F., Zhang, Y., 2013. Rapid photooxidation of As (III) through surface complexation with nascent colloidal ferric hydroxide. Environ. Sci. Technol. 48 (1), 272–278.
Yao, L., Huang, L., He, Z., Zhou, C., Li, G., 2013. Occurrence of arsenic impurities in organoarsenics and animal feeds. J. Agric. Food Chem. 61 (2), 320–324.
Zhu, X.D., Wang, Y.J., Liu, C., Qin, W.X., Zhou, D.M., 2014. Kinetics, intermediates and acute toxicity of arsanilic acid photolysis. Chemosphere 107, 274–281.